Inner Permanent Magnet Synchronous Machine Optimization for HEV Traction Drive Application in Order to Achieve Maximum Torque per Ampere

J. Soleimani*, A. Vahedi* and S. M. Mirimani*

Abstract: Recently, Inner Permanent Magnet (IPM) synchronous machines have been introduced as possible traction motor in hybrid electric vehicle (HEV) and traction applications due to their unique merits. In this machines, in order to achieve maximum torque per ampere (MTPA) by minimum volume of motor, optimization of the motor geometry parameters is necessary. This paper presents a novel structure of IPM synchronous machines for traction applications with fragmental buried rotor magnets in order to achieve low torque ripple, iron losses and cogging torque, furthermore, an iteration method for IPM synchronous machine design is presented to achieve minimum volume, MTPA and low amplitude of cogging torque for this structure. Thus, simulation of this motor is done in order to extract the output values using 3D-Finite Element Method. This method has high accuracy and gives us a better insight of motor performance and presents back EMF, power factor, cogging torque, flux density, torque per ampere diagram, CPSR (constant power speed ratio), torque per speed diagram of this IPM synchronous machine. This study can help designers in design approach of such motors.

Keywords: IPM Synchronous Sachine, Optimal Design, Maximum Torque Per Ampere, Hybrid Electric Vehicle, Traction.

1 Introduction

IPM synchronous machine has many advantages such as high power density, efficiency and wide speed operation, these advantages make it particularly suitable for automotive, traction applications where space, weight and geometry dimensions are very important [1]-[6]. Furthermore, rotor structure and geometry parameters have great impact on torque per ampere diagram, torque ripple, cogging torque and iron losses [3]-[9], so optimal design in order to achieve MTPA and low amplitude of cogging torque and iron losses is necessary. The main feature of IPM synchronous machines for HEV traction drive application is simple construction with conventional three phase stator winding, rotor with inner fragmental Permanent Magnet (PM) [2],[4]-[6], but this paper presents a novel structure of rotor to achieve low torque ripple, iron losses and cogging torque.

The performance of these motors in these applications is quite depending on CPSR which increased by improving the field weakening operation [3]:

$$\text{CPSR} = \frac{\omega_{max}}{\omega_{rated}} \tag{1}$$

Field weakening operation will be improved by increasing the linkage flux between rotor and stator which is increased by increasing the inductance of excitation axis and inductance of excitation axis will be increased by increasing the number of barriers in rotor structure (three barriers maximum) [6], [8]. So, this paper, presents a design method to achieve minimum volume, MTPA and low amplitude of cogging torque for IPM synchronous machines. As a result, presents back EMF, power factor, cogging torque, flux density, torque per ampere diagram, CPSR (constant power speed ratio), torque per speed diagram of this machine. Meanwhile, a 3D-finite element model is implemented in order to simulate IPM synchronous machine, which has high level of accuracy and gives a better insight of motor performance. This model can be used in the design approach and precise analysis of IPM

synchronous machines for HEV traction drive applications.

2 Structure and Winding Configuration

As shown in Fig. 1(a), a 80-kW, 8pole, 48 slots and 6 slots per pole for possible hybrid electric vehicle application (in order to achieve harmonic reduction [10]) IPM synchronous machine has been designed with three layers of fragmental buried rotor magnet (in order to achieve MTPA), but all of these layers have a trapezoid structure as shown in Fig. 1(b) for reduce hot spots (zones that have maximum flux density).

In this machine a kind of permanent magnet material in rotor structure has been used which has suitable reversible temperature coefficients as it can be seen in Table 1 [11]. Also, laminations of permendur-24 for constructing the stator and rotor cores, and a kind of stainless steel with very low relative permeability in shaft structure has been used. Soft magnetic material (permendur-24) characteristics are given in Table 2 [12].

(a)

(b)
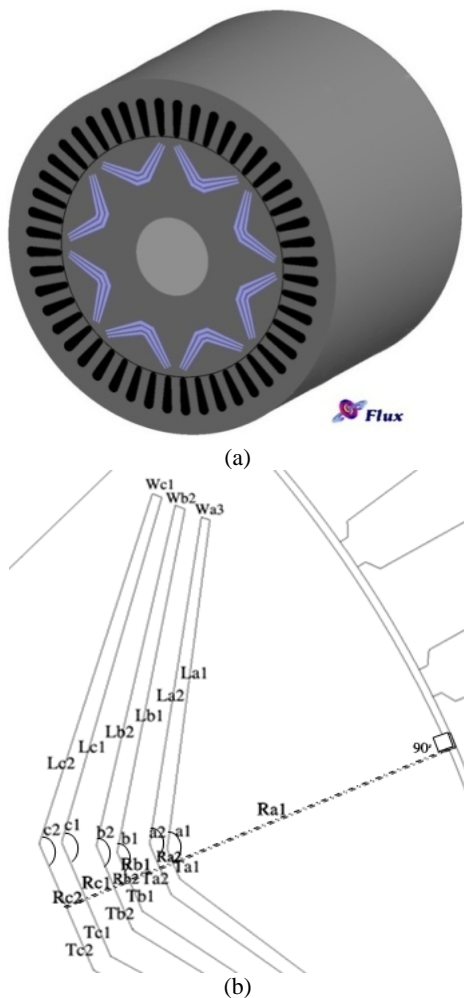
Fig. 1 (a) 8-pole, 48 slot inner permanent magnet synchronous motor structure for traction application with Three layers of fragmental buried rotor magnets, (b) Novel structure of rotor.

Table 1 Permanent magnet characteristics.

Parameters	Sintered Sm_2Co_{17}
B_r (T)	1
H_c (KA/m)	820
μ_r	1.05
T_{max} (°c)	300
T_{ciure} (°c)	750
T_c of B_r	-0.04
T_c of H_c	-0.3

Table 2 Soft magnetic material characteristics.

| Parameters	Permendur-24
Saturation flux density (T)	2.34
Remanence (T)	1.5
Initial permeability	250
maximum permeability	2000

The stator slots are embedded with double layer fractional-slot (5/6) windings with 18 conductors per stator slot and each phase contains eight turns of windings (to achieve harmonic reduction), current density in windings is 4.2 A/mm2 and radius of each naked wire is 2.936 mm by using insulators F-class. The winding diagram and terminal connection mode of the 8-pole stator winding has been shown in Fig. 2. Analysis of model have been performed at one half pole by 3D-finite element method (FEM).

3 FEM Model

As mentioned before, a 3D-finite element model which gives a better insight of motor performance is implemented in order to simulate of proposed motor.

In order to have high level of accuracy the automatic mesh diagram is not used and a mesh diagram is designed manually and node congestion is higher around the air gap. The total number of nodes is about 190000 which lead to high accuracy. Meanwhile, for boundary conditions, the homogenous Dirichlet condition has been adopted on the infinite box that encompasses the motor.

This simulation has been based on circuit coupled model using the phase voltage as input. Fig. 3 shows the circuit coupled model which has been used in this study, for each phase eight coil winding is considered, four coils of them send the current in motor and four coils return current from midpoint of winding in star connection. Coil winding connection in each phase is exactly the same that is illustrated in Fig. 2(b).

(a)

(b)
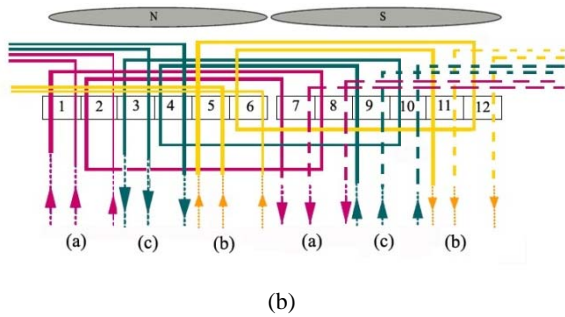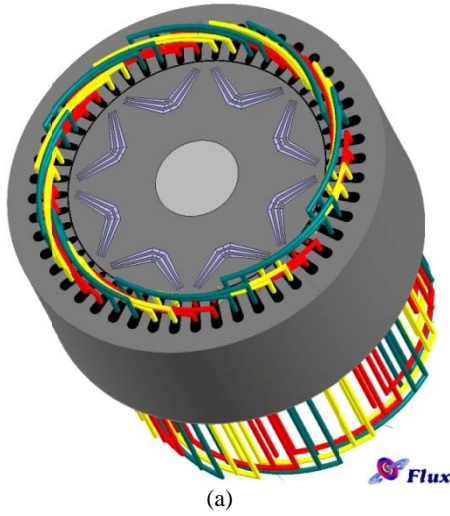
Fig. 2 (a) Winding diagram- (b) A pair pole stator terminal connection of 8-pole IPM synchronous machine with double layer distributed windings.
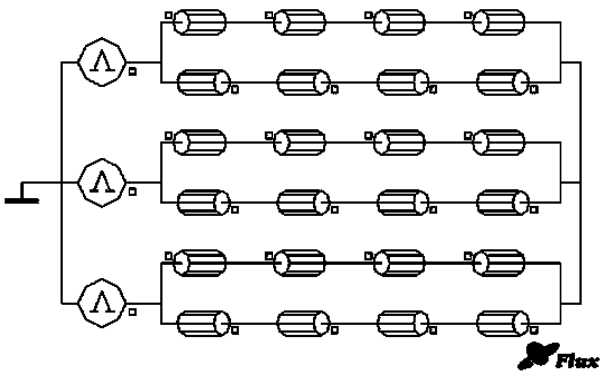
Fig. 3 Circuit coupled model used in simulation.

4 Permanent Magnet Volume

In this study, a complex permeability (the hysteresis loop in the rhombus shape) is used. Fig. 4 helps to exploit this hysteresis loop. In order to choose an accurate volume of permanent magnet regarding to magnetic circuit that PM material is in, an iteration method has been used which illustrated with a flowchart in Fig. 5.

In the first iteration for each type of PM, volume is obtained by using [13]:

$$V_m = \frac{c_v.P_{out}}{F.B_r.H_c} \qquad (2)$$

C_v is a coefficient that depending on the PM design in rotor structure and approximated between 0.54 to 3.1. From the finite element analysis, the back EMF in each phase can be obtained and checked with amplitude of input voltage in each phase and this procedure continues until the convergence criterion will be satisfied. As it can be observed from simulation results, this procedure is so effective for choosing the type and volume of PM with complex permeability and this novel complex structure which has close agreement with real motor tests.
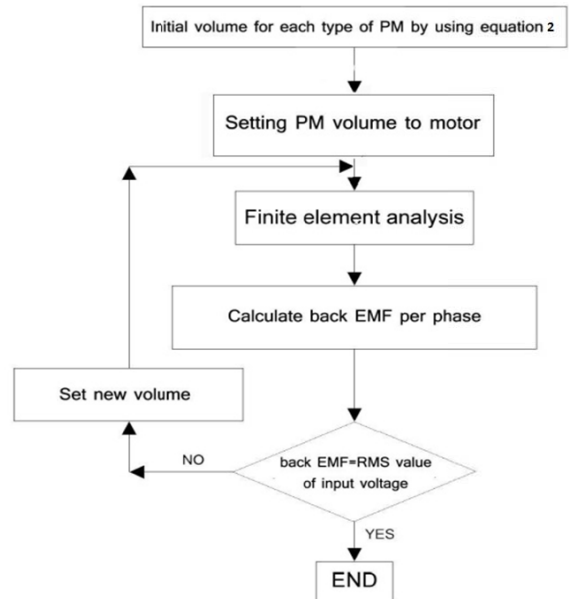
5 Optimal Dimensions Design Method

Basic dimensions of AC machines (axial length and diameter) are obtained by using [14]:

$$D^2.L = \frac{Q}{C_0.n_s} \qquad (3)$$
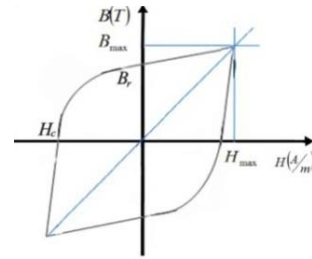
Fig. 4 Inclined hysteresis loop approximation.

Fig. 5 Flowchart for accurate volume of PM selection.

which in this equation, Q is the reactive power, n_s is speed (r.p.s) and C_0 is output coefficient of machine which in the first iteration of flowchart Fig. 6 is obtained by:

$$C_0 = 1.11\pi^2 B_{av} ac K_w 10^{-3}. \tag{4}$$

B_{av} is specific magnetic loading and approximated between 0.35 T to 0.6 T, ac is specific electric loading and approximated between 8000 to 25000 AT/m and k_w demonstrate the winding coefficient.
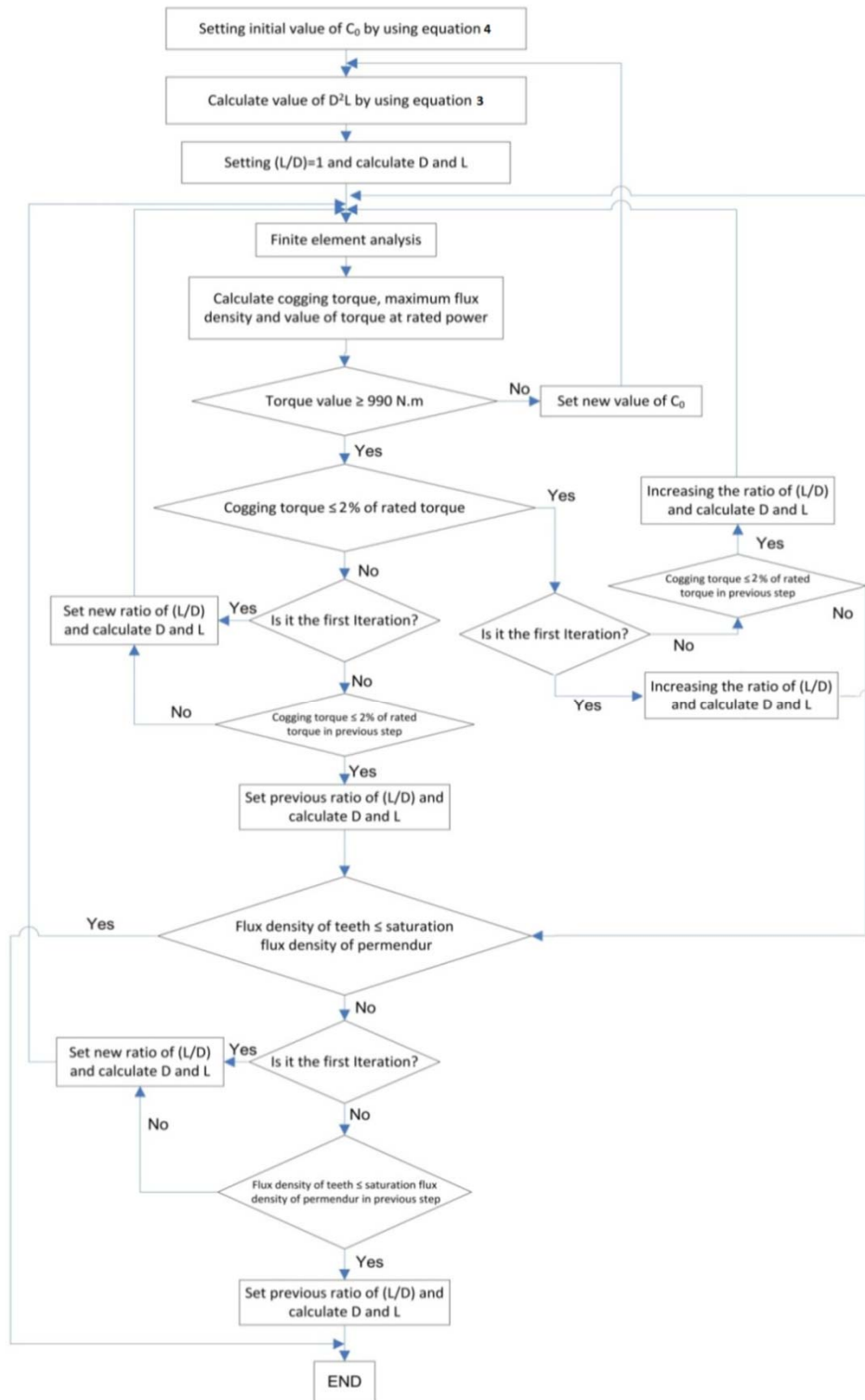
Fig. 6 Iteration method for optimal dimension design.

It's clear that axial length of motor and axial length of PM in IPM synchronous machines are equal to each other and by increasing the inductance of PM, inductance of excitation axis will be improved [4],[15]. Also, it's clear that by increasing the inductance of excitation axis, electromagnetic torque will be improved. Magnetic circuit of a PM and its equivalent electrical circuit are shown in Fig. 7. Equations that demonstrate these terms are as bellow:

$$P_{rc} = \frac{l_m}{\mu_0 \mu_r A_m}. \tag{5}$$

$$F_0 = H_c . l_m. \tag{6}$$

$$\phi_r = B_r A_m. \tag{7}$$

where l_m and A_m respectively are axial length and pole cross section of PM, μ_0 and μ_r respectively denotes permeability of free space and relative permeability of PM [13], so by increasing the axial length of motor, inductance of excitation axis and therefore torque per ampere diagram will be improved [13], [15].
In order to optimal dimension design an iteration method has been used that illustrated with a flowchart in Fig. 6.

The main achievements of this iteration method are:
- Reaching to rated torque more than 990 N.m.
- Reaching to cogging torque less than 2% of rated torque.
  Cogging torque is the consequence of interaction (magnetic attraction) between rotor-mounted permanent- magnets field and the stator teeth, which produces reluctant variations depending on the rotor position; it is stator current independent. It manifests itself by rotor tendency to align with the stator in a number of stable positions (where the permeance of the permanent magnets' magnetic circuit is maximized), even when machine is unexcited, resulting in a pulsating torque, which does not contribute to the net effective torque. Optimizing cogging torque to a low value can be obtained a low torque ripple and harmonic reduction [9]-[11], [16]-[18].
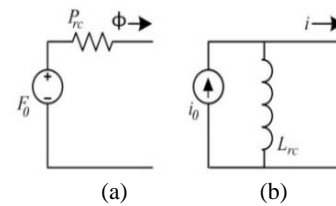
- Flux density of hot spots must be less than saturation flux density of permendur-24.

In this flowchart, in each step, results of flux density in motor structure and cogging torque will be checked, the value of C_0, will be increased step by step in order to achieve minimum volume of machine. For optimization, the ratio of axial length on diameter of motor (L/D) must takes its maximum value until the maximum flux density in hot spots is less than saturation flux density of permendur-24 and amplitude of cogging torque is less than 2% of rated torque.

6 Simulation Results and Discussion

Based on the above respects, finite element simulation for the IPM synchronous machine has been done and the simulation research has been made for the 8 poles IPM synchronous machine. Optimum dimension parameters of the IPM synchronous machine and the output quantities of machine are given in Table 3. It must be noted that one half pole is analyzed because of the magnetic symmetry and alternation of the motor. As it can be seen in Fig. 8, nodes congestion becomes higher near the air gap, in order to accurate simulation. Fig. 9 shows the distribution of flux at rated current. As discusses the sections, flux lines are center of poles and distances between PM and air gap. Fig. 10 shows isovalues diagram of flux density at rated power and as it can be seen from this diagram, maximum flux density is less than saturation flux density of permendur-24 and it's close to the saturation point of this material. Air gap flux density over a predefined path (for 4 poles) has been shown in Fig. 11 at rated power and back EMF for one phase has been shown in Fig. 12. It can be seen, amplitude of back EMF per phase is equal to amplitude of input voltage per phase.

Fig. 7 Magnet's equivalent circuits (a) magnetic circuit (b) electrical circuit.
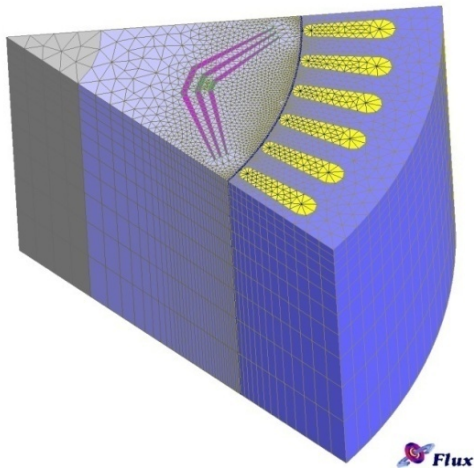
Table 3 Motor features.

Quantity	Value	Quantity	Value
Rated voltage (V)	900	Outer diameter of stator (mm)	734
Rated power (Kw)	80	Inner diameter of stator (mm)	498
Frequency (Hz)	50	Stator stack height (mm)	560
Speed (r.p.m)	750	Type of Winding	Concentric with consequent poles
Phase connection	Y	Number of turns per slot	20
Pole pairs	4	Core material (stator and rotor)	Permendur-24
Number of stator slots	48	Air gap length (mm)	1.6

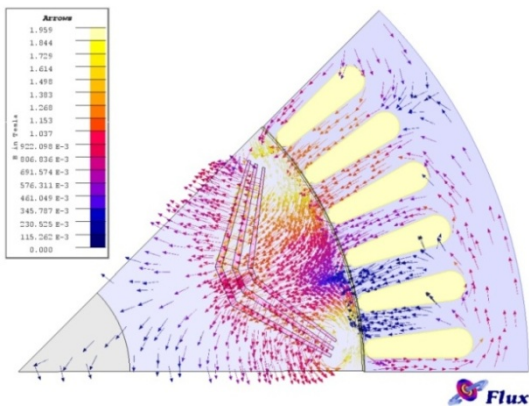**Fig. 8** Mesh diagram of simulated machine.

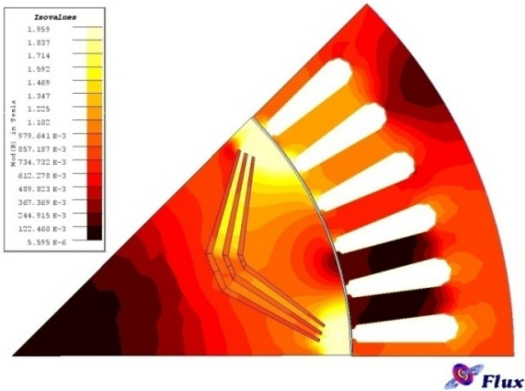**Fig. 9** Distribution of flux at rated current.

Fig. 10 Isovalues diagram of flux density at rated power.

Table 4 verifies suitable performance of this IPM synchronous machine at rated speed. As it can be seen from this table, with this novel structure (trapezoid form fragmental buried magnet), cogging torque is less than 2% of rated torque, but cogging torque in conventional IPM synchronous machines is about 5% of rated torque.
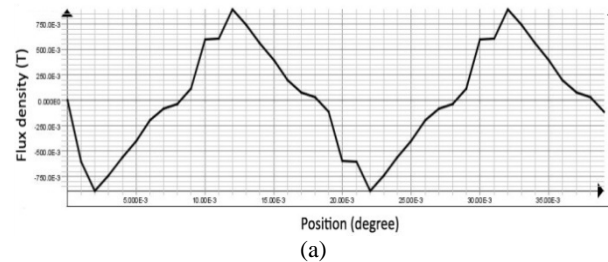
Torque per ampere diagram at maximum and rated speed has been shown in Fig. 13. It can be seen, by increasing the inductance of excitation axis that achieved by increasing the number of barriers in rotor

structure, torque per ampere diagram will be more suitable.

At last, torque per speed diagram has been shown in Fig. 14, and performance of the machine in constant power area of this diagram shows the advantage of this novel structure and authenticity of this iteration method.

Table 4 Optimized IPM synchronous machine performance at rated speed.

Parameters	Optimized IPM synchronous machine
Torque (N.m)	994.1
Cogging torque (N.m)	18.1
Power factor %	97
CPSR	>4
Torque ripple %	4.7
Efficiency %	93.6
Copper loose (w)	2036
Iron loose (w)	3090

(a)

(b)
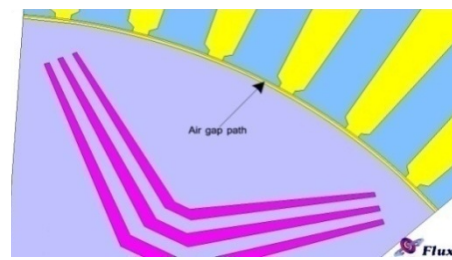
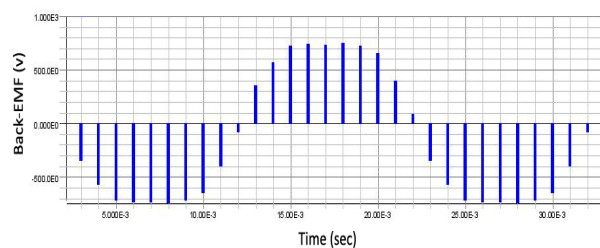**Fig. 11** (b) Air gap flux density diagram over the path (4 pole) (b) Air gap path belong a pole.
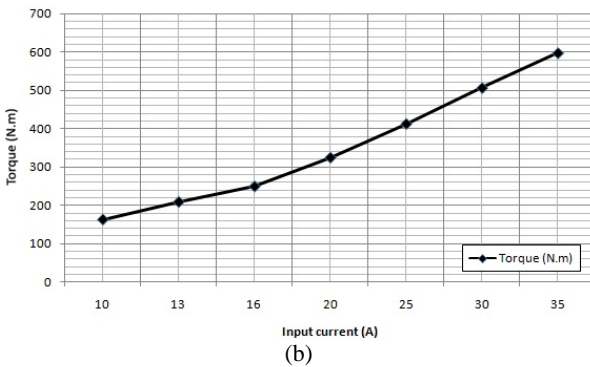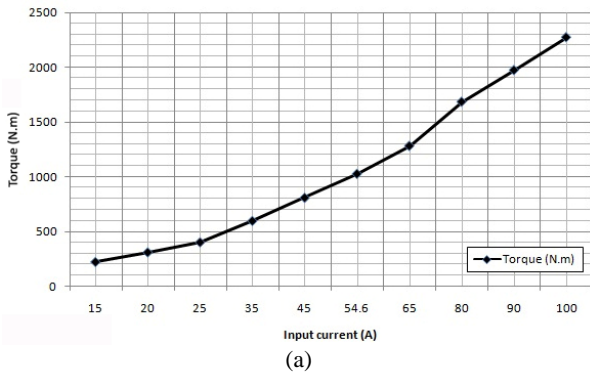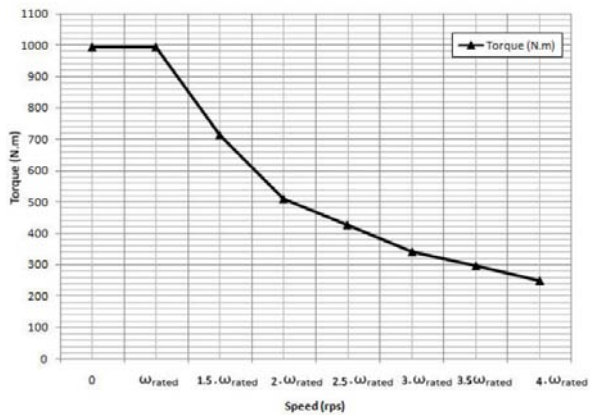

Fig. 12 Back EMF for phase a.

(a)

(b)

Fig. 13 Torque per ampere diagram (a) at rated speed (b) at maximum speed.

Fig. 14 Torque per speed diagram.

7 Conclusion

This paper presents a novel structure of rotor to achieve decreasing the torque ripple, iron losses and cogging torque for IPM synchronous machines. In this structure, 3 layers of PM have been used and each layer has a fragmental trapezoid structure as shown before, with this structure, hot spots (zones that have maximum flux density) will be reduced. Furthermore, in order to optimal dimension design an iteration method has been used that illustrated with a flowchart. The main achievements of this iteration method are reaching to minimum volume, maximum torque per ampere and minimum value of cogging torque by checking the

maximum flux density. The simulation has been done based on optimal dimensions and a 3D-finite element model implemented in order to simulate the IPM synchronous machine, at last presents back EMF, power factor, cogging torque, flux density, torque per ampere diagram, CPSR and torque per speed diagram on this IPM synchronous machine. Simulation results verify the authenticity of this iteration method and advantages of this novel structure. Torque per speed diagram shows the suitable performance of the machine in constant power area, furthermore, cogging torque and torque ripple results and decreasing of the hot spot area shows the advantages of this novel structure. Torque per speed diagram and torque per ampere diagrams shows the increasing the inductance of excitation axis that achieved by increasing the number of barriers in rotor structure and authenticity of this iteration method.

References

[1] Vahedi A. and Ramezani M., "Analysis of Converter-Permanent Magnet Synchronous Machine Set by Iimproved Average-Value Modeling", *Iranian Journal of Electrical & Electronic Engineering* (IJEEE), Vol. 1, No. 2, pp. 81-87, 2005.

[2] Wang A., Li H. and Liu C. T., "On the Material and Temperature Impacts of Interior Permanent Magnet Machine for Electric Vehicle Applications", *IEEE. Trans. on Magnetics*, Vol. 44, No. 11, pp. 4329-4332, Nov. 2008.

[3] Soong W. L. and Ertugrul N., "Field-Weakening Performance of Interior Permanent-Magnet Motors", *IEEE Trans. on Industry Applications*, Vol. 38, No. 5, pp. 1251-1258, Sep./Oct. 2002.

[4] Staunton R. H., Nelson S. C., Otaduy P. J., McKeever J. W., Bailey J. M., Das S. and Smith R. L., "PM Motor Parametric Design Analyses for a Hybrid Electric Vehicle Traction Drive Application", *Oak ridge. National Lab Oak Ridge*, U.S DEP of Energy, pp. 15-39, Sep. 2004.

[5] Fujishima Y., Wakao S., Kondo M. and Terauchi N., "An Optimal Design of Interior Permanent Magnet Synchronous Motor for the Next Generation Commuter Train", *IEEE Trans .on Applied Super conductivity*, Vol. 14, No. 2, pp.1902-1905, Jun 2004.

[6] Honda Y., Nakamura T., Higaki T. and Takeda Y., "Motor Design Considerations and Test Results of an Interior Permanent Magnet Synchronous Motor for Electric Vehicles", *32nd IAS*, New Orleans, LA, pp. 75-82, Oct. 1997.

[7] Woo D. K., Lee S. Y., Seo J. H. and Jung H. K., "Optimal rotor structure design of interior-permanent magnet synchronous machine base on improved niching genetic algorithm", *18th International Conference on Electrical Machines, (ICEM 2008)*, pp.1-4, 2008.

[8] Honda Y., Higaki T., Morimoto S. and Takeda Y., "Rotor design optimization of a multi-layer interior permanent-magnet synchronous motor", *IEE Proc. Electric Power Applications,* Vol. 145, No. 2, pp. 119-124, 1998.

[9] Yamada A., Kawano H., Miki I. and Nakamura M., "A Method of Reducing Torque Ripple in Interior Permanent Magnet Synchronous Motor", *Power Conversion Conference*, pp. 322-325, Nagoya, 2007.

[10] Guemes J. A., Iraolagoitia A. M., Del Hoyo J. I. and Fernandez P., "Torque Analysis in Permanent-Magnet Synchronous Motors", *IEEE. Trans. on Conversion*, Vol. 26, No. 1, pp. 55-63, Mar. 2011.

[11] Widyan M. S., "Design, Optimization, Construction and Test of Rare-Earth Permanent-Magnet Electrical Machines with New Topology for Wind Energy Applications", *Ph.D. dissertation*, Dept. Elect & comp. Eng., Berlin Univ., 2006.

[12] Armco steel Corporation, "The metallurgy of iron and silicon-iron for soft magnetic applications", *technical report*, 2010.

[13] Soleimani J. and Vahedi A., "3-Phase Surface Mounted PMSM Improvement Considering Hard Magnetic Material Type", *International Journal of Advanced Engineering Science and Technologies*, Vol. 7, No. 1, pp. 36-41, Jun. 2011.

[14] Hamdi E. S., *Design of small Electrical machines*, Wiley, John & Sons, Incorporated Inc., USA: New York City, 1995.

[15] Soleimani J., "Permanent Magnet Synchronous Motor Design for Traction Applications" *M.Sc. dissertation, Dept. Electrical Eng*, Iran Univ. of Science & Technology, Tehran, Iran, Sep. 2011.

[16] Lucas C., Gheidari Z. N. and Tootoonchian F., "Using Modular Pole for Multi-Objective Design Optimization of a Linear Permanent Magnet Synchronous Motor by Particle Swarm Optimization (PSO)", *Iranian Journal of Electrical & Electronic Engineering (IJEEE)*, Vol. 6, No. 4, pp. 214-223, 2010.

[17] Lucas C., Tootoonchian F. and Gheidari Z. N., "Multi-Objective Design Optimization of a Linear Brushless Permanent Magnet Motor Using Particle Swarm Optimization (PSO)", *Iranian Journal of Electrical & Electronic Engineering (IJEEE)*, Vol. 6, No. 3, pp. 183-189, 2010.

[18] Jabbari A., Shakeri M. and Nabavi Niaki S. A., "Pole Shape Optimization of permanent magnet synchronous Motors Using the Reduced Basis Technique", *Iranian Journal of Electrical & Electronic Engineering (IJEEE)*, Vol. 6, No. 1, pp. 48-55, 2010.

Javad Soleimani was born in 1985 in Asadabad, Hamedan, Iran. He received the B.S. degree from Bu. Ali. Sina University, Hamedan, Iran and M.Sc. degree from Iran University of Science & Technology (IUST), Tehran, Iran in Power Electrical Engineering respectively in 2007 and 2011. His main research interests include dynamic modeling and application of FEM to design, modeling and optimization of conventional and special electric machines. Also he works on application of power electronics in adjustable speed and torque motor control.

Abolfazl Vahedi was born in Tehran, Iran, in 1966. He received the B.S. degree from Ferdowsi Mashhad University, Mashhad, Iran, in 1989, and the M.Sc. and Ph.D. degrees from the Institut Nationale Polytechnique de Lorraine (INPL), Nancy, France, in 1992 and 1996, respectively, all in electrical engineering. He is currently an Associate Professor and a member of the Center of Excellence for Power System Automation and Operation, Iran University of Science and Technology (IUST), Tehran. He has directed several projects in the area of conventional and special electric machines and drives. His current research interests include design, implementation, and optimization of electric machines & drives. He is a member of the Institution of Electrical Engineers (IEE).

Seyyed Mehdi Mirimani was born in Babol, Iran. He received the B.sc. degree from Mazandaran University of Technology, Babol, Mazandaran, in 2007. He received the M.Sc. degree on the subject of electrical machines in 2010 from Iran University of Science and technology. He is currently working toward the Ph.D. degree in electrical engineering in the Department of Electrical Engineering, Iran University of Science and technology (IUST), Tehran. His research interests include design, modeling, control and finite element analysis of electrical machines and other electromagnetic devices.